Speeding up conditional quantum logic of trapped ion qubits with overlapping pulses

Lachezar S. Simeonov, Peter A. Ivanov, and Nikolay V. Vitanov
Department of Physics, Sofia University, James Bourchier 5 Boulevard, 1164 Sofia, Bulgaria
(Received 11 September 2013; published 6 January 2014)

We introduce two types of two-qubit controlled-phase gates, which operate with trapped ions in a linear Paul trap. Each ion is addressed individually with two sequential bichromatic laser pulses, the two frequency components of which are tuned on exact resonance with the first blue and red vibrational sidebands of the qubit transition frequency. For suitably chosen pulse areas and relative laser phases the dependence on the phonon number vanishes and the net effect is a controlled-phase gate between the electronic qubit states. In contrast to earlier gates, in which the pulses addressing the two ions are separated in time, we use partly overlapping pulses, which make the present gates faster, e.g., by about 26% for rectangular and over 50% for sinusoidal pulses.

DOI: 10.1103/PhysRevA.89.012304 PACS number(s): 03.67.Lx, 03.67.Ac, 37.10.Ty, 32.80.Qk

I. INTRODUCTION

The Sørensen-Mølmer (SM) two-qubit controlled-phase gate [1] is a very popular tool in ion trap quantum computing because, unlike Cirac-Zoller's gate [2–4], it is insensitive to the vibrational motion of the ions and therefore it allows one to work with ions with a nonzero phonon number. Due to this crucial feature, which avoids the need for vibrational ground-state cooling of the ions, the SM gate has been used by numerous ion trapping groups as a kit gate for quantum information processing. The SM gate in a rotated basis was demonstrated by Leibfried *et al*. with 97% fidelity with beryllium ions for a mean phonon number near $\bar{n}=0$ [5]. Later, the SM gate was implemented with 97.4% fidelity with calcium ions in a thermal state of motion with a mean phonon number as large as $\bar{n}=20$ [6]. A record gate fidelity of 99.3% has been achieved by Benhelm *et al*. in another experiment with calcium ions with a mean phonon number close to $\bar{n}=0$ [7]. A phase-stable version of the SM gate has been demonstrated with cadmium ions [8]. The SM gate itself or SM-type interactions have been used to construct a decoherence-free controlled-NOT gate [9], to entangle two- and four-ion qubits [10], to create up to 14-qubit Greenberger-Horne-Zeilinger (GHZ) states [11,12], Toffoli gate [13], cluster states [14], to implement quantum error correction [15], digital quantum simulations [16,17], etc.

The SM gate uses a bichromatic laser field, the two frequencies of which are tuned at a certain detuning $\delta=2\pi/T$ from the respective red and blue sidebands, where T is the pulse duration. This condition slows down the gate because of certain upper limits on δ set by the trap. Several gates have been proposed which overcome this limitation [18–23]. Milburn, Schneider, and James (MSJ) [18] proposed to use constant resonant Hamiltonians H_1 and H_2, applied sequentially upon ions 1 and 2, respectively, as follows: $e^{iH_1t}e^{iH_2t}e^{-iH_1t}e^{-iH_2t}$. They showed that a spin-spin interaction can be achieved if H_1 and H_2 are of the type $\lambda_1 J_k P$ and $\lambda_2 J_k X$, where P and X are momentum and position operators, and k denotes the component of the spin J; then the propagator becomes $e^{-i\lambda_1\lambda_2 J_k^2 T^2}$.

In this paper, we propose a physical implementation of the MSJ gate using bichromatic laser pulses. Unlike the SM gate [19], the lasers are now tuned on *exact* resonance with the first blue and red sidebands, and therefore this implementation of the MSJ gate is faster. In addition, we propose to accelerate this two-qubit c-phase gate by using partly *overlapping* bichromatic laser pulses. We show that there is an optimal pulse overlap, which minimizes the necessary pulse area and therefore increases the speed of the gate. We calculate the gate duration explicitly for rectangular and powers-of-sine pulse shapes; the gate speeds up by as much as 26% for rectangular shapes and over 50% for sine-shaped pulses. We show first how the c-phase gate is constructed with two ions and a single mode of oscillation, and then we generalize the gate to the multimode case, for an arbitrary number N of ions in the trap.

II. BACKGROUND: SINGLE MODE

A. Single set of bichromatic pulses

We consider a linear ion crystal of N ions, aligned along the z axis. Each ion has two internal states $|\uparrow\rangle$ and $|\downarrow\rangle$, which compose the qubit, with a Bohr transition frequency ω_0. The interaction-free Hamiltonian of the system is (assuming $\hbar=1$ hereafter)

$$H_0=\sum_{k=1}^{N}\frac{\omega_0}{2}\sigma_k^z+\sum_{n=1}^{N}\omega_n a_n^\dagger a_n, \tag{1}$$

where σ_k^q $(q=x,y,z)$ denotes the qth Pauli matrix for ion k. $a_n^\dagger$ and a_n are the creation and annihilation operators of the nth collective vibrational mode of the ion chain with a frequency ω_n. We assume that each ion interacts with a pair of laser fields along the transverse x direction with laser frequencies $\omega_r=\omega_0-\omega_n$ and $\omega_b=\omega_0+\omega_n$, tuned at the red- and blue-sideband resonances, respectively, of the selected nth vibrational mode. Because at the moment we are interested in the single-mode case, we omit hereafter the index n of the mode for the sake of simplicity; we will return to it in the multimode case. In the optical rotating-wave approximation, the interaction Hamiltonian in the Lamb-Dicke limit is given by [8,24–27]

$$H(t)=\sum_{k=1}^{N}g_k(t)\sigma(\phi_k^+)(a^\dagger e^{-i\phi_k^-}+ae^{i\phi_k^-}), \tag{2}$$

where $g_k(t)$ is the time-dependent Rabi frequency of the individual spin-phonon coupling and $\sigma(\phi_k^+)=e^{-i\phi_k^+}\sigma_k^+ +$

$e^{i\phi_k^+}\sigma_k^-$, with σ_k^+ (σ_k^-) being the spin raising (lowering) operator for ion k. The spin and motional laser phases are defined by $\phi_k^+ = \frac{1}{2}(\phi_k^{\rm b} + \phi_k^{\rm r})$ and $\phi_k^- = \frac{1}{2}(\phi_k^{\rm b} - \phi_k^{\rm r})$, where $\phi_k^{\rm b}$ and $\phi_k^{\rm r}$ are the laser phases of the blue- and red-detuned laser beams, respectively. Hereafter, we set $\phi_k^- = \phi_k$ and we assume that $\phi_k^+ = 0$, hence $\sigma(\phi_k^+) = \sigma_k^x$.

By using the Magnus formula for the propagator [28–31],

$$U(t,t_i) = \exp\left\{-i\int_{t_i}^{t} dt_1 H_1 - \frac{1}{2}\int_{t_i}^{t} dt_1 \int_{t_i}^{t_1} dt_2 [H_1,H_2] + \frac{1}{6} i \int_{t_i}^{t} dt_1 \int_{t_i}^{t_1} dt_2 \int_{t_i}^{t_2} dt_3 ([H_1,[H_2,H_3]] + [H_3,[H_2,H_1]]) + \cdots\right\}, \tag{3}$$

with $H_l \equiv H(t_l)$, and by noticing that the third-order and all higher-order terms in it vanish, it is straightforward to show that

$$U(t,t_i) = D(\alpha)\exp\left[i\sum_{k<l}^{N} J_{k,l}\sigma_k^x\sigma_l^x\right], \tag{4}$$

where $D(\alpha) = e^{\alpha a^\dagger - \alpha^\dagger a}$ is the displacement operator and

$$\alpha(t,t_i) = -i\sum_{k=1}^{N} A_k(t,t_i)e^{-i\phi_k}\sigma_k^x, \tag{5a}$$

$$J_{k,l}(t,t_i) = \sin(\phi_k - \phi_l)\int_{t_i}^{t} dt_1 \int_{t_i}^{t_1} dt_2 [g_k(t_2)g_l(t_1) - g_k(t_1)g_l(t_2)], \tag{5b}$$

where $A_k(t,t_i) = \int_{t_i}^{t} dt_1 g_k(t_1)$ is the temporal pulse area of the laser pulse at the position of ion k.

It is very important that in the propagator (4) the vibrational motion is factored out into the displacement operator, whereas the other factor depends on the internal motion only. The key idea here is to annul the displacement, i.e., to make $\alpha = 0$, without killing the internal-motion factor. However, this cannot be achieved with the application of a single pair of pulses on the gate qubits because they would have to have the same time dependence; then the commutator in Eq. (5b) would vanish, too. From another perspective, since the laser field is on resonance with the respective vibrational mode frequency, it excites the motional state, which, however, does not follow a circular path in the position-momentum space, as for a detuned laser field.

B. Two pairs of bichromatic pulses

In order to return the vibrational state to its initial state, we apply a second bichromatic pair of laser pulses. Then, the total unitary propagator is given by

$$U(t,t_i) = D(\alpha'')D(\alpha')\exp\left[i\sum_{k<l}^{N}(J'_{k,l} + J''_{k,l})\sigma_k^x\sigma_l^x\right], \tag{6}$$

with the total displacement

$$D(\alpha'')D(\alpha') = e^{\frac{1}{2}(\alpha''\alpha''^\dagger - \alpha'\alpha'^\dagger)}e^{-\alpha''^\dagger a}e^{(\alpha''+\alpha')a^\dagger}e^{-\alpha'^\dagger a}, \tag{7}$$

where the symbols $'$ and $''$ denote quantities related to the first and second pairs of pulses, respectively. We find that the total displacement returns the motional state to its initial state if

$$\sum_{k=1}^{N}(A'_k e^{-i\phi'_k} + A''_k e^{-i\phi''_k}) = 0. \tag{8}$$

Then the propagator becomes

$$U(t,t_i) = \exp\left[i\sum_{k<l}^{N}(J'_{k,l} + J''_{k,l})\sigma_k^x\sigma_l^x\right], \tag{9}$$

which acts only upon the internal ion states; no motional vibrations are excited at the end of the pulse sequence.

Condition (8) can be satisfied for equal pulse areas,

$$A'_k = A''_k \quad (k = 1,2,\ldots,N), \tag{10a}$$

and laser phases

$$\phi'_k = \phi''_k - \pi \quad (k = 1,2,\ldots,N). \tag{10b}$$

Then $J'_{k,l} = J''_{k,l}$ and Eq. (9) becomes

$$U(t,t_i) = \exp\left[2i\sum_{k<l}^{N} J'_{k,l}\sigma_k^x\sigma_l^x\right]. \tag{11}$$

It is very important that condition (8) leaves a freedom to shape the spin-phonon couplings in a such a way that the spin-spin couplings (5b) do not vanish at the end of the pulse sequence. Therefore the propagator of Eq. (11) makes it possible to design conditional quantum logic gates.

III. *c*-PHASE GATE WITH TWO IONS

A. General framework

As an example, we consider the case of two ions, $N = 2$. The propagator (11) reads

$$U(t,t_i) = \exp\left[2iJ'_{1,2}\sigma_1^x\sigma_2^x\right]. \tag{12}$$

Obviously, for

$$J'_{1,2} = \pi/8 \tag{13}$$

this propagator reduces to

$$U = \exp\left(i\frac{\pi}{4}\sigma_1^x\sigma_2^x\right), \tag{14}$$

which, apart from a global phase and a local phase transformation [5], is the c-phase gate in the rotated basis $|\pm\rangle = (|\uparrow\rangle \pm |\downarrow\rangle)/\sqrt{2}$. Hence our discussion now focuses on the fulfillment of the condition (13).

Because $J'_{1,2}$ is proportional to the squared pulse duration, it is appropriate to set the sine factor in Eq. (5b) to unity; this requires $\phi'_1 - \phi'_2 = \pi/2$. The phases therefore must satisfy

$$\phi'_2 = \phi'_1 - \pi/2, \tag{15a}$$

$$\phi''_1 = \phi'_1 + \pi, \tag{15b}$$

$$\phi''_2 = \phi'_1 + \pi/2. \tag{15c}$$

The phase ϕ'_1 is arbitrary; it is related to the unimportant global phase and can be set to zero.

Condition (13) now reduces to

$$\int_{t_i}^{t_f} dt_1 \int_{t_i}^{t_1} dt_2 [g_1(t_2)g_2(t_1) - g_1(t_1)g_2(t_2)] = \frac{\pi}{8}. \quad (16)$$

The left-hand side of this equation can be written as

$$g_1^0 g_2^0 T^2 G(\tau/T) = \frac{\pi}{8}, \quad (17)$$

where the function $G(\tau/T)$ depends on the pulse shape and the pulse delay τ, while g_1^0 and g_2^0 are the maximum values of the couplings applied on qubits 1 and 2. As we showed in Eq. (10a), the couplings for the two pairs of pulses must be equal, therefore we drop the symbols $'$ and $''$. Because we aim to maximize the gate speed, we take $g_1^0 = g_2^0 \equiv g^0$. We stress here that, unlike the SM gate, this equality of the couplings is not mandatory; different couplings can be used as well, leading to a slight increase in the gate duration. For the sake of simplicity, we also assume that all pulses have the same shape $g(t)$, although applied at different times, as shown in Fig. 1.

Condition (17) is a condition for an effective pulse area $g^0 T\sqrt{G(\tau/T)}$. In order to have the fastest possible gate, we have to take the largest possible value of the Rabi frequency g^0. The latter is usually limited by the trap features, e.g., by the relevant trap frequency and the frequency mode. Therefore it is appropriate to assume that g^0 is set and fixed to its largest allowed value, and our objective now is to find out how to arrange the pulses such that the gate duration is minimized. To this end, we emphasize again that the function $G(\tau/T)$ depends on both the pulse delay τ and the pulse shape $g(t)$. Next, we take particular pulse shapes $g(t)$ and we determine the optimal delay, which produces the shortest gate duration. It is easy to see that the delay τ cannot be set naively to zero because then the commutator in Eq. (16) vanishes. There is an optimum value τ_0 of the delay, for which the gate duration $2T + 2\tau$ is minimal; its determination is a simple exercise in calculus.

We note that because we fixed the peak Rabi frequency g^0, the pulse duration T becomes a variable: It is determined from condition (16), which depends on the pulse shape and the pulse delay. Therefore the pulse width is a function of the pulse shape and the delay: $T \to T(\tau)$.

Equation (16) is valid when the two pairs of bichromatic pulses do not overlap, as in the MSJ gate and our gate of type I described below. If these pairs overlap, as in our gate of type II presented below, instead of Eq. (16) we should use

$$\int_{t_i}^{t_f} dt_1 \int_{t_i}^{t_1} dt_2 [g_1(t_2)g_2(t_1) - g_1(t_1)g_2(t_2)] = \frac{\pi}{4}. \quad (18)$$

Here $g_k(t)$ is the overall Rabi frequency of the sequence of two bichromatic pulses addressing ion k ($k = 1,2$), while t_i and t_f mark the initial and final times of the entire gate.

B. MSJ gate

We begin with the case when the pulses do not overlap (MSJ gate). We use temporally separated pulses, $\tau = T$. Then Eq. (16) reduces to $A^2 = \frac{\pi}{8}$, where $A = \int_0^T g(t)dt$ is the pulse area of each pulse, i.e.,

$$A = \sqrt{\frac{\pi}{8}}. \quad (19)$$

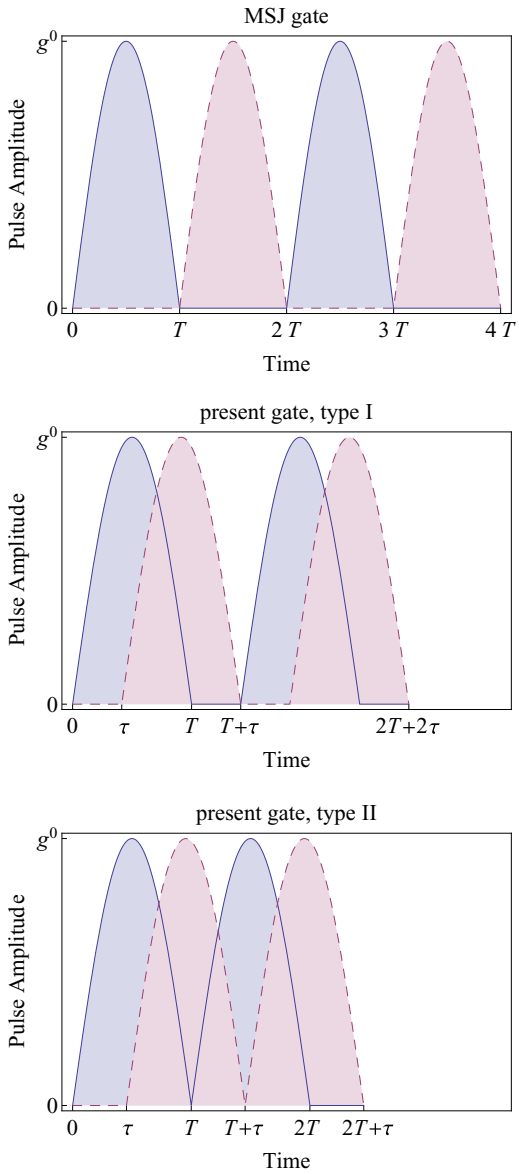

FIG. 1. (Color online) Pulse ordering for the controlled-phase gate with sinusoidal pulse shapes, $g(t) = g^0 \sin(\pi t/T)$. Solid curves show the pulses applied on the controlled qubit 1 and dashed curves show the pulses on the target qubit 2. Top frame: Temporally separated pulses applied alternatively upon qubits 1 and 2 (MSJ gate), with gate duration $4T$. Middle frame: Two separated pairs of temporally overlapped pulses (present gate, type I), with gate duration $2T + 2\tau_0$, where τ_0 is the optimal delay, for which the gate duration is minimal. Bottom frame: Overlapped pairs of overlapped pulses (present gate, type II), with gate duration $2T + \tau_0$. Note that the pulse durations for type-I and type-II gates are slightly longer than for the MSJ gate; however, due to the pulse overlap the total gate durations are shorter.

The total gate duration is $4T$ [see Fig. 1 (upper frame)]. For rectangular, $g(t) = g^0$, and power-of-sine pulses, $g(t) = g^0 \sin^n(\pi t/T)$ $(0 \leqq t \leqq T)$, the total gate duration reads, respectively, $\mathcal{T}_{\rm MSJ} = \sqrt{2\pi}/g^0$ for rectangular pulses, $\mathcal{T}_{\rm MSJ} = \pi\sqrt{\pi/2}/g^0$ for sine pulses, $\mathcal{T}_{\rm MSJ} = 2\sqrt{2\pi}/g^0$ for $\sin^2$ pulses, etc. We shall use these MSJ gate durations as reference values for the comparison with our two gates in Table I.

TABLE I. Comparison of the parameters of the gates of types I and II presented here and the MSJ gate for rectangular, $g(t) = g^0$, and power-of-sine pulses, $g(t) = g^0 \sin^n(\pi t/T)$ $(0 \leqq t \leqq T)$. For the MSJ gate ($\tau = T$), the gate duration is $\mathscr{T}_{\rm MSJ} = 4T$. For our gate of type I the gate duration is $\mathscr{T}_I = 2T + 2\tau$, and for our gate of type II the gate duration is $\mathscr{T}_{II} = 2T + \tau$. The peak Rabi frequency g^0 is fixed; the pulse duration T is given in units $1/g^0$. The speedup is calculated as the total duration of the MSJ gate $\mathscr{T}_{\rm MSJ}$ divided by the total duration $\mathscr{T}_I$ or $\mathscr{T}_{II}$ of the corresponding gate of type I or II.

Pulse	MSJ gate	Present gate: Type I			Present gate: Type II		
shape	T	τ/T	T	Speedup	τ/T	T	Speedup
rect	0.627	0.500	0.724	15.5%	0.500	0.793	26.5%
sin	0.984	0.413	1.094	27.3%	0.454	1.091	47.1%
$\sin^2$	1.253	0.362	1.370	34.4%	0.424	1.327	55.8%
$\sin^3$	1.477	0.327	1.597	39.3%	0.393	1.539	60.4%
$\sin^4$	1.671	0.303	1.794	43.0%	0.365	1.731	63.3%
$\sin^5$	1.846	0.284	1.971	45.9%	0.341	1.905	65.5%
$\sin^6$	2.005	0.268	2.131	48.4%	0.321	2.065	67.3%

The phase point of the MSJ gate describes a closed path in the position-momentum space as shown in the top frame of Fig. 2. Unlike the SM gate, this is achieved by a simple change of the laser phases, rather than by tuning the lasers off resonance with the first sidebands.

Our implementation of the MSJ gate, using bichromatic lasers on *exact* resonance with the first red and blue sidebands, is faster than the SM gate by a factor $\sqrt{\pi/2}$, i.e., by over 25%, without requiring additional experimental resources for physical implementation. In addition, it leaves a leeway for further improvement using partly overlapping pulses, as described below.

C. Accelerated c-phase gate of type I

By letting the pulses overlap partly, as shown in the middle frame of Fig. 1, we can now design a faster gate which has a shorter duration than the MSJ gate. There are two separate pulse pairs, within each of which a pulse applied to qubit 1 is overlapped with a pulse on qubit 2, with a time delay τ. The total gate duration is $\mathscr{T}_I(\tau) = 2T(\tau) + 2\tau$, where the pulse width $T(\tau)$ is calculated from Eq. (16). The minimization of $\mathscr{T}_I(\tau)$ requires $d\mathscr{T}_I(\tau)/d\tau = 0$, which amounts to solving the equation $dT(\tau)/d\tau = -1$.

1. Rectangular pulses

For rectangular pulses the calculation is simple and explicit. Equation (16) reads

$$2\tau T(\tau) - \tau^2 = \frac{\pi}{8(g^0)^2}. \tag{20}$$

We determine $T(\tau)$ from here and then we find the minimum of the gate duration $\mathscr{T}_I(\tau) = 2T(\tau) + 2\tau$; it occurs at $\tau_0 = 0.5T$. Then we find from Eq. (20) that $T = \sqrt{\pi/6}/g^0$. The optimal (minimal) gate duration is $\mathscr{T}_I = 2(T + \tau_0) = 3T$, or

$$\mathscr{T}_I = \frac{\sqrt{6\pi}}{2g^0} = \frac{\sqrt{3}}{2}\mathscr{T}_{\rm MSJ}. \tag{21}$$

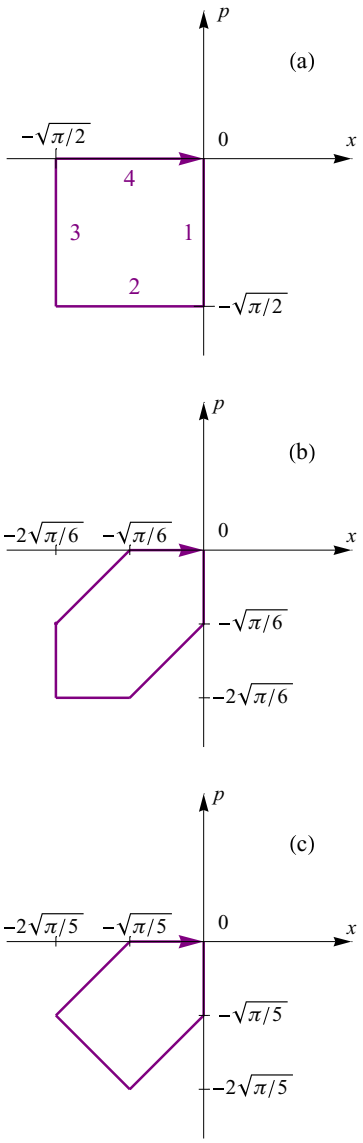

FIG. 2. (Color online) Closed paths in the phase space of the three gates described here: (a) MSJ gate; (b) gate of type I; (c) gate of type II. We have assumed rectangular pulse shapes. We have introduced the dimensionless position and momentum: $x = a + a^\dagger$ and $p = i(a^\dagger - a)$.

Therefore our gate duration $\mathscr{T}_I$ is 86.6% of the MSJ duration $\mathscr{T}_{\rm MSJ}$, which implies a speedup of 15.5% over the MSJ gate. In the middle frame of Fig. 2 the closed path of the phase point of gate of type I is displayed in the position-momentum space.

2. Sinusoidal pulse shapes

The explicit calculation of the double integral in Eq. (16) produces, for most pulse shapes, transcendental equations for $T(\tau)$, which cannot be solved explicitly. Fortunately, such a solution is not needed because it suffices to differentiate Eq. (16) with respect to τ and set $dT(\tau)/d\tau = -1$ in it. Then the resulting equation for τ/T is solved numerically.

For $g(t) = g^0 \sin(\pi t/T)$ $(0 \leqq t \leqq T)$ Eq. (16) reads

$$4T^2(\tau)\sin^2\frac{\pi\tau}{2T(\tau)} + \pi T(\tau)[T(\tau)-\tau]\sin\frac{\pi\tau}{T(\tau)} = \frac{\pi^3}{8(g^0)^2}. \tag{22}$$

We differentiate this equation with respect to τ and set $dT(\tau)/d\tau = -1$. Then we find numerically $\tau_0 = 0.413T$ and $T = 1.094/g^0$. The gate duration is

$$\mathscr{T}_I = \frac{3.093}{g^0} = 0.786\mathscr{T}_{\rm MSJ}. \tag{23}$$

Therefore this gate is faster by over 27% than the MSJ gate.

In the same manner we have calculated the optimized gate parameters for $\sin^n$ pulse shapes, with $n > 1$. The results are presented in Table I.

We have included sinusoidal pulses here because they have certain advantages over rectangular shapes [32]. Compared to rectangular pulses, $\sin^n$ pulses demand, of course, larger duration T for the same pulse area (cf. the increase of T with n in Table I). However, because they are much more adiabatic than rectangular pulses, they exhibit greatly reduced power broadening; therefore, $\sin^n$ pulses allow one to use larger peak Rabi frequencies g^0 without affecting neighboring states. The use of higher g^0 can compensate the increased duration for $\sin^n$ pulses: It has been found that the values $n = 1$–3 provide the largest speedup in certain systems [32].

D. Accelerated *c*-phase gate (type II)

We have found out that the c-phase gate can be accelerated further by letting the pulses overlap even more, as shown in the bottom frame of Fig. 1. The two sequential pulses on qubit 1 are applied right next to each other, without a delay, and the same applies to the two sequential pulses on qubit 2. The two-pulse sequence on ion 2 is delayed with respect to the one on qubit 1 by a delay τ [cf. Fig. 1 (bottom frame)]. The phase relations between the pulses are the same as above, Eqs. (15). We note that a further overlap, e.g., on the two sequential pulses applied on ion qubit 1 (or 2), is not beneficial because the phase relations (15) imply that in the overlap area the fields cancel and have no effect.

The optimal delay is calculated similarly to the type-I gate. However, the total gate duration now is $\mathscr{T}_{II}(\tau) = 2T(\tau) + \tau$. The minimization of $\mathscr{T}_{II}(\tau)$ requires $d\mathscr{T}_{II}(\tau)/d\tau = 0$, which now amounts to solving the equation $dT(\tau)/d\tau = -1/2$. We have calculated the optimized gate parameters for rectangular and $\sin^n$ pulse shapes; the results are presented in Table I.

Because of the greater pulse overlap, the type-II gate is even faster than the type-I gate, at the expense of a slightly increased complexity of the implementation. Compared to the reference MSJ gate, the type-II gate is faster by 26.5% for rectangular pulses, 47% for sine pulses, and over 50% for $\sin^n$ pulses. In the bottom frame of Fig. 2 the phase trajectory of the present gate of type II is displayed.

We note that the gate of Garcia-Ripoll, Zoller, and Cirac [21] is theoretically faster than our gates. However, its speedup comes at the expense of the increased complexity and exponentially increased sensitivity to variations in the interaction parameters. The physical implementation of the MSJ gate and the gates of type I and II, proposed here, can be achieved with essentially the same experimental resources as the SM gate.

IV. MULTIPLE MODES

Now we account for the existence of multiple modes. We assume that the bichromatic laser frequencies $\omega_{\rm b,r} = \omega_0 \pm \mu$ are shifted from the carrier frequency ω_0 with a detuning μ. We will show that, despite the presence of other modes, the two pairs of bichromatic laser pulses still produce the desired c-phase gate.

The interaction Hamiltonian is given by [33]

$$H = \sum_{k,n=1}^{N} g_{kn}(t)\sin(\mu t)\sigma_k^x[a_n^\dagger e^{i(\omega_n t-\phi_k)} + a_n e^{-i(\omega_n t-\phi_k)}], \tag{24}$$

where the index n numbers the modes and the index k numbers the ion qubits. By using the Magnus formula (3), we find the propagator of this Hamiltonian,

$$U(t,t_i) = \exp\left[\sum_{k,l=1}^{N}(L_{kl} + iK_{kl})\sigma_k^x\sigma_l^x\right]\prod_{n=1}^{N}e^{\beta_n a_n^\dagger}\prod_{m=1}^{N}e^{-\beta_m^\dagger a_m}, \tag{25}$$

where

$$L_{kl} = -\frac{1}{2}\sum_{n=1}^{N}B_{kn}B_{ln}^* e^{i(\phi_l-\phi_k)}, \tag{26a}$$

$$K_{kl} = \sum_{n=1}^{N}\int_{t_i}^{t}dt_1\int_{t_i}^{t_1}dt_2 g_{kn}(t_1)g_{ln}(t_2)\sin(\mu t_1)\sin(\mu t_2) \times \sin[\phi_l - \phi_k + \omega_n(t_1-t_2)]. \tag{26b}$$

We have defined the pulse area B_{kn} and the displacement β_n as

$$B_{kn} = \int_{t_i}^{t} g_{kn}(t_1)\sin(\mu t_1)e^{i\omega_n t_1}dt_1, \tag{27a}$$

$$\beta_n = -i\sum_{k=1}^{N}B_{kn}\sigma_k^x e^{-i\phi_k}. \tag{27b}$$

The laser fields excite all vibrational modes, which, as in the single-mode case above, can be reversed to the initial state by a second pair of bichromatic fields. For a sequence of two bichromatic pulse pairs the propagator reads

$$U(t,t_i) = \exp\left[\sum_{k,l}(L'_{kl} + L''_{kl} + iK'_{kl} + iK''_{kl})\sigma_k^x\sigma_l^x\right] \times e^{-\sum_m \beta_m'^\dagger\beta_m''}\prod_n e^{(\beta'_n+\beta''_n)a_n^\dagger}\prod_m e^{-(\beta_m'^\dagger+\beta_m''^\dagger)a_m}. \tag{28}$$

Similarly to the single-mode case, the displacement vanishes if

$$B'_{kn} = B''_{kn}, \quad \phi'_k = \phi''_k + \pi \quad (k,n = 1,\ldots,N). \tag{29}$$

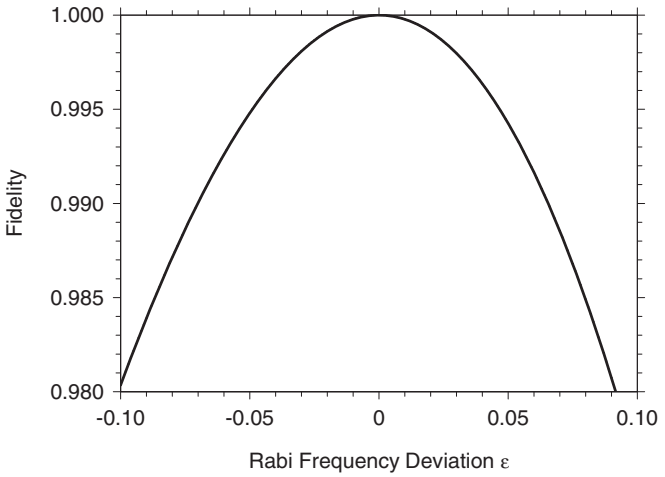

FIG. 3. Fidelity as a function of the deviation ε of the couplings $g_k(t) = g_k^0(1+\varepsilon)f(t)$ for the implementation of the c-phase gate.

Then

$$U(t,t_i) = \exp\left[i \sum_{k,l=1}^{N} (K'_{kl} + K''_{kl})\sigma_k^x \sigma_l^x \right]. \qquad (30)$$

V. PRACTICAL CONSIDERATIONS

One of the major sources of error during the gate operation arises from the nonvanishing coupling to the spectator vibrational modes. In our gate implementation conditions (10) and (29) ensure that all modes return to their initial states. These conditions are crucial and are a major source of infidelity. An important advantage of our technique is that as long as the laser beams addressing the respective ion are derived from the same laser source, the intensity and phase fluctuations are common; then the intensity and phase fluctuations will make all couplings and phases increase and decrease simultaneously, and thereby the conditions (10) remain valid. Hence, at the final moment t_f, the phase point would have described a closed path in the phase space and no additional phonons would be excited. Here we discuss the effects of laser intensity fluctuations, which ruin the perfect operation of the gate due to spoiling of condition (17).

If the initial qubit state is $|\Psi_0\rangle$, the final state would be $|\Psi_f\rangle = U|\Psi_0\rangle$ after a perfect evolution. We assume that the phonon modes are initially in a thermal state and the qubit is in a pure state, which evolves into a state, described by the density operator $\rho = \mathrm{Tr}_{\mathrm{ph}}[U(t_f)|\Psi_0\rangle\langle\Psi_0|U^\dagger(t_f)]$. The difference between the ideal state $|\Psi_f\rangle$ and the final state described by ρ defines the fidelity $F(t) = \overline{\langle\Psi_f|\rho|\Psi_f\rangle}$. The overbar means averaging upon all possible initial qubit states, equivalent to averaging through the angles in the Bloch spheres of the two ions. In Fig. 3 we show the fidelity in the preparation of the c-phase gate as a function of the uncertainty ε in the value of the couplings g_k^0. Since we assume that the fluctuations in the couplings are simultaneous for all ions, the resulting fidelity decreases quadratically with ε.

Finally, we note that the gate scheme proposed here can be implemented also by using a magnetic field gradient and microwave fields, instead of lasers [34–37]. Indeed, the required spin-phonon coupling (2), which is usually induced by optical fields, can be implemented by using microwave radiation and a magnetic field gradient. Such a gate realization has a particular advantage because of the easier individual addressing of the ions in the frequency space [38].

On the other hand, using magnetic-field-sensitive states as a qubit could decrease the coherence time due to fluctuations of the magnetic field. However, such fluctuations can be suppressed with the assistance of a strong carrier microwave field, which decouples the qubit states from the external magnetic field noise [36,37,39,40]. This additional carrier field does not spoil the gate operation but only gives an additional phase factor, which can be removed, e.g., by dynamical decoupling [41].

VI. CONCLUSIONS

In this paper, we have proposed a physical implementation of the MSJ gate, by application of bichromatic laser pulses tuned on exact resonance with the first blue and red sidebands of the carrier qubit frequency. As a special case, we have introduced a two-qubit conditional phase gate, which operates in a linear Paul ion trap and does not depend on the vibrational state of the ion chain and the number of ions. This c-phase gate uses two sequential (identical but phase-shifted) pairs of resonant bichromatic laser pulses to address the two ion qubits. In each pair, one of the bichromatic pulses addresses the control qubit and the other addresses the target qubit, with the two pulses being delayed but partly overlapped in time. We have found the existence of an optimal delay τ_0 between the pulses, for which the gate duration is shortest. We have calculated the pulse parameters for several pulse shapes, given in Table I, with a speedup over the MSJ gate (hitherto the fastest c-phase gate) ranging from 26% for rectangular pulses to over 50% for sinusoidal pulses. Although for simplicity we have assumed equal couplings for the control and target qubits, this equality of the couplings is not mandatory (unlike the SM gate); different couplings can be used with a slight increase of the gate duration. We have shown that this gate operates equally well for any number of ions and normal modes of vibration.

ACKNOWLEDGMENT

This work has been supported by the Bulgarian NSF Grant No. DMU-03/107 and the EC Seventh Framework Programme under Grant Agreement No. 270843 (iQIT).

[1] A. Sørensen and K. Mølmer, Phys. Rev. Lett. **82**, 1971 (1999).
[2] J. I. Cirac and P. Zoller, Phys. Rev. Lett. **74**, 4091 (1995).
[3] C. Monroe, D. M. Meekhof, B. E. King, W. M. Itano, and D. J. Wineland, Phys. Rev. Lett. **75**, 4714 (1995).
[4] F. Schmidt-Kaler, H. Häffner, M. Riebe, S. Gulde, G. P. T. Lancaster, T. Deuschle, C. Becher, C. F. Roos, J. Eschner, and R. Blatt, Nature (London) **422**, 408 (2003).

[5] D. Leibfried, B. DeMarco, V. Meyer, D. Lucas, M. Barrett, J. Britton, W. M. Itano, B. Jelenkovic, C. Langer, T. Rosenband, and D. J. Wineland, Nature (London) **422**, 412 (2003).
[6] G. Kirchmair, J. Benhelm, F. Zahringer, R. Gerritsma, C. F. Roos, and R. Blatt, New J. Phys. **11**, 023002 (2009).
[7] J. Benhelm, G. Kirchmair, C. F. Roos, and R. Blatt, Nat. Phys. **4**, 463 (2008).
[8] P. C. Haljan, K.-A. Brickman, L. Deslauriers, P. J. Lee, and C. Monroe, Phys, Rev. Lett. **94**, 153602 (2005).
[9] T. Monz, K. Kim, A. S. Villar, P. Schindler, M. Chwalla, M. Riebe, C. F. Roos, H. Häffner, W. Hänsel, M. Hennrich, and R. Blatt, Phys. Rev. Lett. **103**, 200503 (2009).
[10] C. A. Sackett, D. Kielpinski, B. E. King, C. Langer, V. Meyer, C. J. Myatt, M. Rowe, Q. A. Turchette, W. M. Itano, D. J. Wineland, and C. Monroe, Nature (London) **404**, 256 (2000).
[11] T. Monz, P. Schindler, J. T. Barreiro, M. Chwalla, D. Nigg, W. A. Coish, M. Harlander, W. Hänsel, M. Hennrich, and R. Blatt, Phys. Rev. Lett. **106**, 130506 (2011).
[12] K. Mølmer and A. Sørensen, Phys. Rev. Lett. **82**, 1835 (1999).
[13] T. Monz, K. Kim, W. Hänsel, M. Riebe, A. S. Villar, P. Schindler, M. Chwalla, M. Hennrich, and R. Blatt, Phys. Rev. Lett. **102**, 040501 (2009).
[14] P. A. Ivanov, N. V. Vitanov, and M. B. Plenio, Phys. Rev. A **78**, 012323 (2008).
[15] P. Schindler, J. T. Barreiro, T. Monz, V. Nebendahl, D. Nigg, M. Chwalla, M. Hennrich, and R. Blatt, Science **332**, 1059 (2011).
[16] B. P. Lanyon, C. Hempel, D. Nigg, M. Muller, R. Gerritsma, F. Zahringer, P. Schindler, J. T. Barreiro, M. Rambach, G. Kirchmair, M. Hennrich, P. Zoller, R. Blatt, and C. F. Roos, Science **334**, 57 (2011).
[17] R. Blatt and C. F. Roos, Nat. Phys. **8**, 277 (2012).
[18] G. J. Milburn, S. Schneider, and D. F. V. James, Fortschr. Phys. **48**, 801 (2000).
[19] A. Sørensen and K. Mølmer, Phys. Rev. A **62**, 022311 (2000).
[20] D. Jonathan and M. B. Plenio, Phys. Rev. Lett. **87**, 127901 (2001).
[21] J. J. Garcia-Ripoll, P. Zoller, and J. I. Cirac, Phys. Rev. Lett. **91**, 157901 (2003).
[22] L.-M. Duan, Phys. Rev. Lett. **93**, 100502 (2004).
[23] S.-L. Zhu, C. Monroe, and L.-M. Duan, Europhys. Lett. **73**, 485 (2006).
[24] D. J. Wineland, C. Monroe, W. M. Itano, D. Leibfried, B. E. King, and D. M. Meekhof, J. Res. Natl. Inst. Stand. Technol. **103**, 259 (1998).
[25] P. J. Lee, K.-A. Brickman, L. Deslauriers, P. C. Haljan, L.-M. Duan, and C. Monroe, J. Opt. B: Quantum Semiclass. Opt. **7**, 371 (2005).
[26] C. Schneider, D. Porras, and T. Schaetz, Rep. Prog. Phys. **74**, 024401 (2012).
[27] D. J. Wineland, Rev. Mod. Phys. **85**, 1103 (2013).
[28] W. Magnus, Commun. Pure Appl. Math. **7**, 649 (1954).
[29] P. Pechukas and J. C. Light, J. Chem. Phys. **44**, 3897 (1966).
[30] R. M. Wilcox, J. Math. Phys. **8**, 962 (1967).
[31] S. Blanes, F. Casas, J. A. Oteo, and J. Ros, Eur. J. Phys. **31**, 907 (2010).
[32] I. I. Boradjiev and N. V. Vitanov, Phys. Rev. A **88**, 013402 (2013).
[33] K. Kim, M.-S. Chang, R. Islam, S. Korenblit, L.-M. Duan, and C. Monroe, Phys. Rev. Lett. **103**, 120502 (2009).
[34] F. Mintert and C. Wunderlich, Phys. Rev. Lett. **87**, 257904 (2001).
[35] A. Khromova, C. Piltz, B. Scharfenberger, T. F. Gloger, M. Johanning, A. F. Varon, and C. Wunderlich, Phys. Rev. Lett. **108**, 220502 (2012).
[36] N. Timoney, I. Baumgart, M. Johanning, A. F. Varon, M. B. Plenio, A. Retzker, and C. Wunderlich, Nature (London) **476**, 185 (2011).
[37] S. C. Webster, S. Weidt, K. Lake, J. J. McLoughlin, and W. K. Hensinger, Phys. Rev. Lett. **111**, 140501 (2013).
[38] M. Johanning, A. Braun, N. Timoney, V. Elman, W. Neuhauser, and C. Wunderlich, Phys. Rev. Lett. **102**, 073004 (2009).
[39] S.-B. Zheng, Phys. Rev. A **66**, 060303(R) (2002).
[40] A. Bermudez, P. O. Schmidt, M. B. Plenio, and A. Retzker, Phys. Rev. A **85**, 040302(R) (2012).
[41] T. R. Tan, J. P. Gaebler, R. Bowler, Y. Lin, J. D. Jost, D. Leibfried, and D. J. Wineland, Phys. Rev. Lett. **110**, 263002 (2013).